Supporting Information

Atomic Layer Deposition of TiO_2 Shells on MoO_3 Nanobelts Allowing Enhanced Lithium Storage Performance

Sanmu Xie,[a,†] Daxian Cao,[a,†] Yiyi She,[b] Hongkang Wang,[a,*] Jianwen Shi,[a] Micheal K H Leung,[b] Chunming Niu[a]

[a] *Center of Nanomaterials for Renewable Energy (CNRE), State Key Lab of Electrical Insulation and Power Equipment, School of Electrical Engineering, Xi'an Jiaotong University, Xi'an 710049, P. R. China*

[b] *Ability R&D Energy Research Centre (AERC), School of Energy and Environment, City University of Hong Kong, Hong Kong SAR.*

[†] *These authors contribute equally to this work.*

*Corresponding author: hongkang.wang@mail.xjtu.edu.cn

Experimental Section

Material synthesis.

Synthesis of MoO_3 nanobelts. MoO_3 nanobelts were synthesized *via* hydrothermal method. In a typical synthesis, 2.0 g ammonium molybdate powder was first dissolved in 30 mL deionized water under magnetic stirring to form a clear solution. Afterwards, 10 mL nitrogen acid was added into by drop-by-drop under continuous stirring for 2 h. The mixture was then transferred to a Teflon lined stainless steel autoclave, which was kept at 180 ^oC for 24 h. After naturally cooling down to room temperature, MoO_3 nanobelts were obtained after washing with distilled water and ethanol for several times, which were then dried at 80 ^oC for 12 h in the oven.

Atomic layer deposition (ALD) of TiO_2 layers on MoO_3 nanobelts. A home-made ALD system (Figure S1) was used for the deposition of TiO_2 layers on MoO_3 nanobelts. In a typical ALD cycle, MoO_3 nanobelts in vacuum were alternately exposed into the $TiCl_4$ and H_2O gases, thus the atomic layer adsorption of $TiCl_4$ and H_2O can react on the surface of MoO_3, producing an atomic layer of TiO_2. Desired thickness of TiO_2 shells can be obtained by repeating the ALD cycle (Figure S2).

Materials Characterization.

Powder X-ray diffraction (XRD) patterns of the products were obtained on a Bruker D2 PHASER X-ray diffractometer using Cu Kα radiation (λ = 1.5418 A) with an operating voltage of 30 kV and a current of 10 mA. Scanning electron microscope (SEM) was performed on an FEI Quanta 250 SEM. Transmission electron microscope (TEM) and high-resolution TEM (HRTEM) were carried out on a JEOL JEM2100 TEM operated at 200 kV. Energy-dispersive X-ray spectroscopy (EDS) was performed on JEM-F200 Field Emission TEM instrument. X-ray photoelectron spectroscopy (XPS) was performed on a Thermo Fisher ESCALAB 250Xi instrument. All the binding energies were calibrated by referring to the C 1s peak at 284.6 eV.

Electrochemical Measurements.

Electrochemical properties were examined using CR2025 coin-type cells assembled in an Ar-filled glovebox with both H_2O and O_2 content less than 1.0 ppm. The working electrode was prepared by casting aqueous slurry consisted of active material, acetylene black and polyacrylic acid (PAA) binder with a weight ratio of 80:10:10, followed by drying at 120 °C under vacuum overnight. Lithium foil was used as the counter electrode, and microporous membrane (Celgard 2400) was used as the separator. An electrolyte containing 1 M $LiPF_6$ dissolved in a mixture of ethylene carbonate/dimethyl carbonate with a volume ratio of 1:1. Galvanostatic discharge/charge tests of the cells were carried out on a battery test system (NEWARE BTS, Neware Technology Co., Ltd., China) in the range of 0.01-3.0 V (vs. Li/Li^+) at room temperature (25 °C). Cyclic voltammetry (CV) was carried out on an electrochemical station (Autolab PGSTAT 302 N) in the range of 0.01-3.0 V at a scan rate of 0.2 mV/s. Electrochemical impedance spectroscopy (EIS) was performed in the frequency range of 10 MHz-0.01 Hz with a voltage amplitude of 5 mV using CHI600E electrochemical station. The specific capacities were based on the mass of the active materials with average loading amount of approximately 1.0 mg/cm^2.

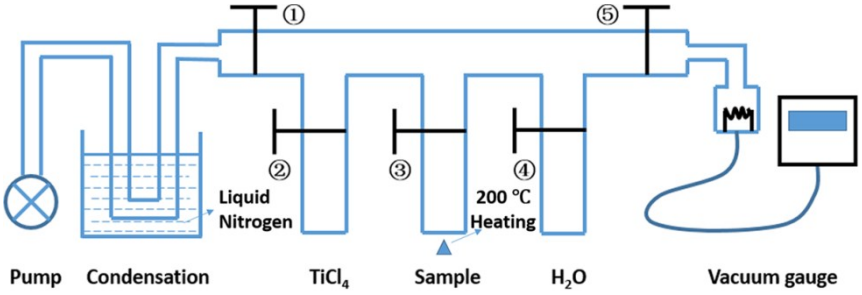

An ALD cycle
- Step 1: Open the valves ①②③④⑤ for 10 min.
- Step 2: Close ①②④ ⑤.
- Step 3: Open ② for 10s, and close
- Step 4: Open ① for 10s, and close
- Step 5: Open ③ for 10s, and close
- Step 6: Open ① for 10s, and close

Figure S1. Schematic illustration of the home-made ALD setup and the ALD cycling process.

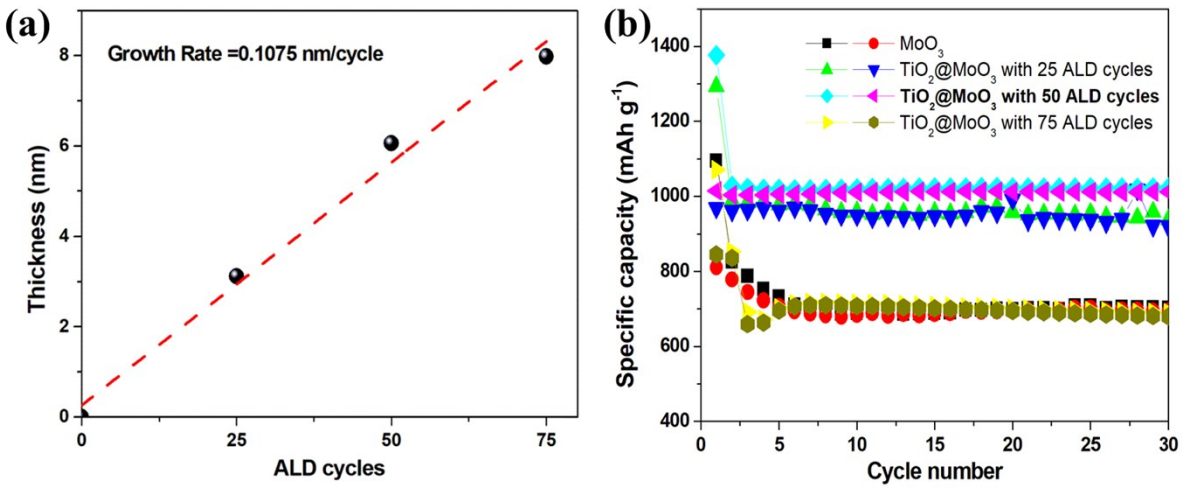

Figure S2. (a) Relationship of TiO_2 thickness along with ALD cycle numbers, and (b) the effect of ALD cycles on the electrochemical properties of TiO_2@MoO_3.

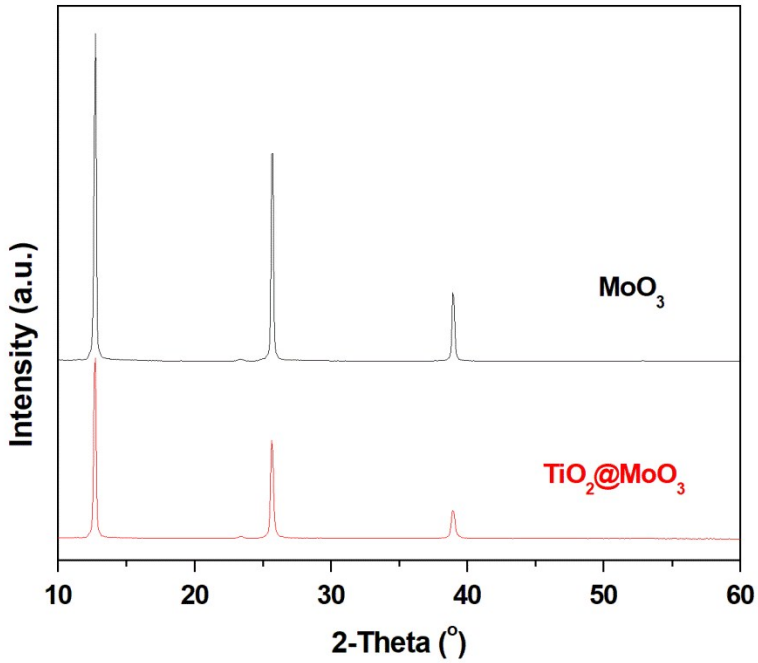

Figure S3. XRD patterns of the the MoO_3 and TiO_2@MoO_3 nanobelts.

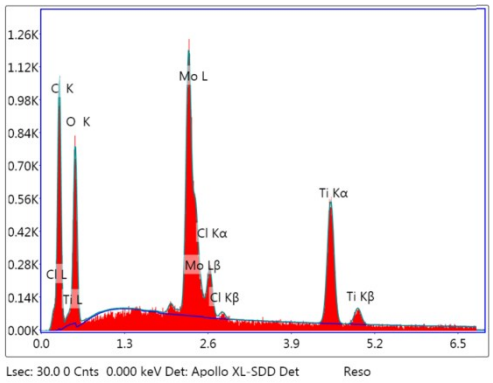

Figure S4. EDS spectrum of TiO_2@MoO_3 nanobelts.

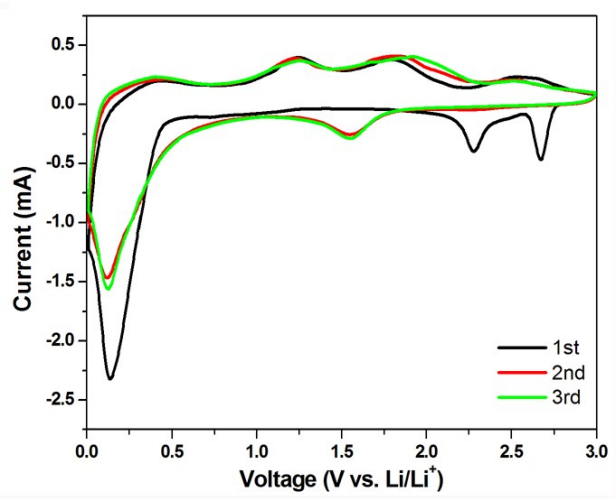

Figure S5. CV curves of the commercial MoO_3 (Macklin, AR, 99.5%).

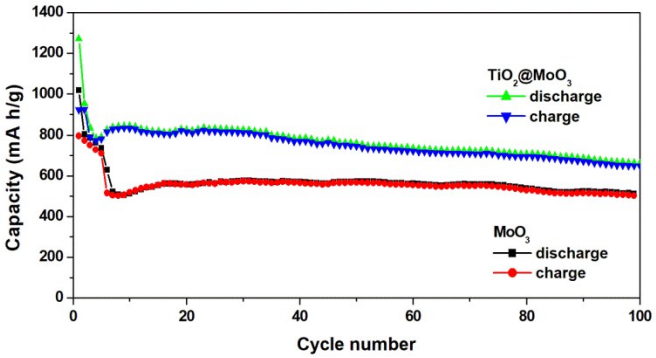

Figure S6. Cycle performance of the MoO_3 and TiO_2@MoO_3 at a high-rate of 1 A g^{-1}. For MoO_3 electrode, a lower current density was applied in the first five cycles.

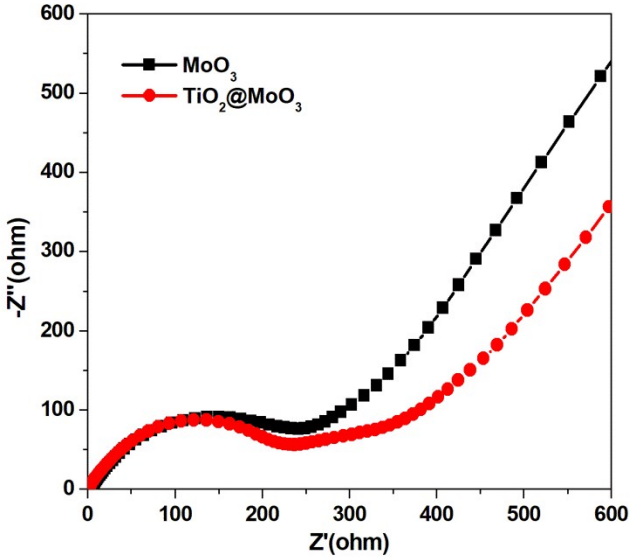

Figure S7. Nyquist plots of the MoO_3 and TiO_2@MoO_3 electrodes before cycling.